African Journal of Advanced Pure and Applied Sciences (AJAPAS)
Online ISSN: 2957-644X
Volume 4, Issue 4, 2025
Page No: 259-267
Website: https://aaasjournals.com/index.php/ajapas/index
ISI 2025: 1.126 SJIFactor 2024: 6.752 معامل التأثير العربي: 1.62

Numerical and Experimental Analysis of (HE10) Hydrous Ethanol Blend in a PFI Gasoline Engine

Musaab O. El-Faroug [1,2]*, Salem A. Basher [2]
[1] Mechanical Engineering Department, Faculty of Engineering, Elimam Elmahdi University, Sudan
[2] Faculty of Energy and Mining Engineering, Sirte University, Libya

التحليل العددي والتجريبي لخليط الإيثانول المائي (*HE10*) في محرك بنزين بحقن الوقود في المنفذ

مصعب عمر الفاروق مبارك جعفر [2,1]*، سالم عبدالعالي بشير [2]،
[1] قسم الهندسة الميكانيكية، كلية الهندسة، جامعة الامام المهدي، كوستي، السودان
[2] كلية هندسة الطاقة والتعدين، جامعة سرت، سرت، ليبيا

*Corresponding author: musaabgaffar@gmail.com

Received: August 12, 2025	Accepted: October 16, 2025	Published: October 25, 2025

Abstract:
This work examines the effects of 10% hydrous ethanol–gasoline blends (HE10) on the combustion and emission behavior of a spark-ignition port fuel injection (PFI) engine. Numerical simulations using a CFD solver evaluated the role of water content in blends (E0, HE10W3, HE10W5) on in-cylinder pressure, heat release rate, and NOx formation at 1200 rpm and 50 N·m. Experimental tests were also carried out on a four-cylinder PFI gasoline engine at 1800 rpm under different loads to assess the influence of HE10 on particulate matter (PM) and gaseous emissions. The results indicate that hydrous ethanol blends reduce peak in-cylinder pressure and heat release compared with gasoline, mainly due to higher latent heat of vaporization and lower heating value. Nonetheless, HE10 provided clear emission advantages. PM number and mass concentrations declined substantially, with a 64.9% reduction in particulate mass at 30 N·m relative to gasoline, and particle size distributions showed fewer nucleation and accumulation mode particles. In addition, HE10 lowered NOx, HC, CO, and CO_2 emissions. A slight increase in brake-specific fuel consumption was observed, reflecting the lower energy density of hydrous ethanol.

Keywords: Port injection gasoline engine, CFD software, experiment, hydrous ethanol, Combustion characteristics, emissions.

الملخص
يهدف هذا العمل إلى دراسة تأثير خلطات الإيثانول المائي بنسبة 10% مع البنزين (HE10) على سلوك الاحتراق والانبعاثات في محرك اشتعال بالشرارة مزوّد بحقن وقود عند صمام الدخول (PFI). تم إجراء محاكاة عددية باستخدام برنامج ديناميكا الموائع الحسابية (CFD) لتقييم دور محتوى الماء في الخلطات (E0، HE10W3، HE10W5) على ضغط الأسطوانة، معدل انطلاق الحرارة، وتكوين أكاسيد النيتروجين (NOx) عند سرعة 1200 دورة/دقيقة وحمل 50 نيوتن·متر. كما أُجريت اختبارات عملية على محرك بنزين رباعي الأسطوانات من نوع PFI عند سرعة 1800 دورة/دقيقة وأحمال مختلفة لتقييم تأثير HE10 على الجسيمات الصلبة (PM) والانبعاثات الغازية. أظهرت النتائج أن خلطات الإيثانول المائي تخفض ضغط الأسطوانة الأقصى ومعدل انطلاق الحرارة مقارنة بالبنزين، ويُعزى ذلك أساساً إلى ارتفاع الحرارة الكامنة للتبخر وانخفاض القيمة الحرارية. ومع ذلك، قدّم وقود HE10 مزايا واضحة من حيث الانبعاثات؛ إذ انخفض عدد الجسيمات وكتلتها بشكل ملحوظ، حيث سُجّل انخفاض بنسبة 64.9% في كتلة الجسيمات عند حمل 30 نيوتن·متر مقارنة بالبنزين، كما أظهرت توزيعات حجم الجسيمات انخفاضاً في الجسيمات الناتجة عن طور النواة وطور التراكم. إضافةً إلى

ذلك، أدى HE10 إلى خفض انبعاثات NOx وHC وCO وCO_2. ولوحظت زيادة طفيفة في الاستهلاك النوعي للوقود بالفرملة، وهو ما يُعزى إلى انخفاض الكثافة الطاقية للإيثانول المائي.

الكلمات المفتاحية: محرك بنزين بحقن عند صمام الدخول، برمجيات ديناميكا الموائع الحسابية (CFD)، تجربة، إيثانول مائي، خصائص الاحتراق، الانبعاثات.

1. Introduction

The rapid pace of industrialization has created a growing demand for energy sources that are not only abundant and renewable but also environmentally sustainable. At the same time, emissions from automobiles remain a major contributor to air pollution, particularly haze formation, and pose significant risks to human health. Among potential biofuels to replace gasoline, alcohols are considered the most promising candidates. Ethanol, in particular, is already widely utilized worldwide [1]. The production of anhydrous ethanol (with a water content below 1%) is energy-intensive and costly, primarily due to the distillation and dehydration processes required. Notably, the removal of the final 5% of water demands disproportionately high energy input. Consequently, the direct utilization of hydrous ethanol as a fuel can markedly enhance overall energy efficiency, thereby strengthening its viability as a sustainable fuel alternative [2-6]. Hydrous ethanol possesses several advantages over conventional gasoline, making it an attractive alternative fuel. It is characterized by a low carbon-to-hydrogen ratio, high octane number, lower toxicity, wider flammability limits, and faster burning velocity. In addition, its high latent heat of vaporization reduces intake air temperature, thereby enhancing engine power output and volumetric efficiency. Owing to these favorable combustion properties, hydrous ethanol represents a promising and environmentally friendly substitute for automotive applications [6] . The application of ethanol–gasoline–water blends as alternative fuels is associated with certain limitations. In particular, the high latent heat of vaporization of ethanol reduces fuel volatility, which poses challenges under cold weather conditions and can result in difficulties during cold engine start-up [7].

The use of biofuels has become a widely adopted strategy to reduce greenhouse gas emissions and lessen dependence on fossil fuels. Internal combustion (IC) engines primarily emit nitrogen oxides (NOx), carbon dioxide (CO2), carbon monoxide (CO), hydrocarbons (HC), and particulate matter (PM). These emissions are of significant concern due to their detrimental effects on both the environment and human health. Consequently, increasingly stringent emission regulations are being enforced on IC engines. Particulate matter (PM) emissions have gained significant attention due to studies showing that even low-to-moderate exposure from IC engines adversely affects human health [8, 9]. Health impacts are more strongly linked to particle size than mass [10], with smaller particles from gasoline engines posing greater respiratory risks than larger diesel-derived particles [11]. NOx formation primarily depends on burnt gas temperature, residence time at high temperature, excess oxygen, and turbulence [12]. Longer exposure of the combustion gases to high temperatures leads to increased NOx production. HC, CO, and CO_2 are primary emissions from IC engines, arising mainly from incomplete fuel combustion, fuel evaporation, and fuel properties [12, 13]. HC and CO contribute to air pollution and can cause adverse health effects, such as respiratory irritation and cardiovascular disorders [14], whereas CO_2 is a major greenhouse gas responsible for climate change [15].

Our previous review [1] indicates that hydrous ethanol is a renewable and cost-effective alternative fuel for spark-ignition engines. Its unique chemical and physical properties relative to gasoline enhance combustion and engine performance while reducing CO, NOx, HC, and CO_2 emissions, although unregulated emissions such as acetaldehyde and formaldehyde may rise. The temperature-dependent stability and water solubility of ethanol–gasoline blends are also addressed. Lou et al. [6] investigated hydrous ethanol–gasoline blends in a four-cylinder PFI engine operating at 2000 rpm under different loads. The results indicated that gasoline produced the highest peak in-cylinder pressure, whereas hydrous ethanol blends led to reductions in PM, NOx, and HC emissions, with particle numbers decreasing as load increased. Overall, the study highlights hydrous ethanol as a promising alternative fuel for mitigating engine emissions. . Wang et al. [16] investigated the effects of HE20 (20% hydrous ethanol–gasoline) on cycle-to-cycle variation in a PFI spark-ignition engine under various speeds and loads. The findings indicated that HE20 lowered variation at low loads compared to gasoline, showed poorer stability than E20 at 1600 rpm, but enhanced combustion stability over both E20 and E0 at 2000 rpm.

Rufino et al. [17] investigated hydrous ethanol combustion in a flex-fuel engine using heat release analysis under different speeds, loads, ignition timings, and lean air–fuel ratios. The study showed that, compared to gasoline, ethanol exhibited shorter combustion duration, lower knock sensitivity, and smaller Wiebe exponent values, offering valuable data for simplified combustion modeling. Ambros et al. [18] evaluated commercial hydrous ethanol blends containing 10–40% water by volume in an SI engine with fixed ignition timing. The study found that higher water content increased the pressure at the end of the compression stroke, while overall in-cylinder pressure declined as water concentration in the fuel rose. Catapano et al. [19] investigated gasoline–ethanol blends under both PFI and DI conditions using in-cylinder thermodynamic analysis and reported that the ethanol evaporation cooling effect was more pronounced in DI operation. Schifter et al. [2] examined mid-level gasoline–ethanol blends (10–40%) in a single-cylinder SI engine and found that hydrous ethanol increased in-cylinder pressure and reduced intake temperatures compared to anhydrous blends, while also lowering combustion speed, heat release rate, and NOx emissions. Melo et al. [20] tested hydrous ethanol–gasoline blends in a 1.4 L flex-fuel FIAT engine and found that hydrous ethanol allowed advanced spark timing without knock, leading to higher peak pressures. It also reduced CO, NOx, and HC emissions, though CO_2 increased due to ethanol's chemical composition.

Shi et al. [21] conducted three-dimensional CONVERGE simulations of hydrous ethanol–gasoline combustion in a direct-injection engine with EGR. Increasing ethanol content enhanced flame propagation, shortened combustion duration, and reduced soot formation by up to 73% relative to pure gasoline. The combination of EGR with hydrous ethanol further improved combustion, lowered in-cylinder temperatures, and decreased NOx, PAH, and soot emissions. Martins [22] conducted a numerical study on the effect of spark plug electrode gaps on E96W4 and E100 ethanol combustion in a DI SI engine using Star-CD. The models were validated against experimental thermodynamic data and high-speed imaging, offering insights into flame propagation, combustion stability, and the influence of spark plug configuration on engine performance and emissions. Willems [23] developed a CFD model of an RCCI engine fueled with E85/diesel to study the influence of injection timing, boost pressure, intake temperature, and spray angle on combustion, stratification, heat loss, and emissions. The study found that injection timing governs fuel stratification, boost pressure affects combustion timing and NOx formation, intake temperature alters HRR and combustion duration, and spray angle together with piston geometry shapes flame structure and unburned hydrocarbon emissions. Gandolfo et al. [24] examined the impact of injection pressure on a split-injection SI strategy using hydrous ethanol (92% ethanol, 8% water). Higher injection pressures (200 bar) enhanced combustion efficiency, reduced knock intensity by up to 90%, and permitted greater spark advance, while the relative timing of intake and compression stroke injections affected knock suppression.

This study used a commercial computational fluid dynamic (CFD) to numerically assess the influence of water content in ethanol–gasoline blends (E0, HE10W3(3% water), HE10W5(5% water)) on in-cylinder pressure, heat release rate, and NOx at 1200 rpm and 50 Nm. Experimentally, HE10W5 effects on in-cylinder pressure, heat release, particulate matter, and gaseous emissions (NOx, CO, CO_2, HC) were evaluated in a port-injection gasoline engine at 1800 rpm under different loads.

2. Material and methods

2.1 Numerical simulation and method

In this study, the SAGE chemistry solver [25] was employed to couple detailed chemical kinetics with the combustion simulations, computing reaction rates alongside the CFD transport equations. NO_x formation was modeled using the extended Zeldovich mechanism [26]. CFD simulations were carried out using a skeletal chemical kinetic model. The gasoline surrogate mechanism developed by Liu et al. [27] incorporates isooctane, n-heptane, and toluene, comprising 56 species and 168 reactions. Ethanol kinetics were adopted from [28] and integrated into the surrogate model with minor modifications to improve predictions of ignition delay and combustion characteristics. The resulting mechanism for ethanol–gasoline blends includes 62 species and 194 reactions, representing the combustion of ethanol, toluene, n-heptane, and isooctane.

2.2 Experimental setup and method

2.2.1 Test engine and fuels

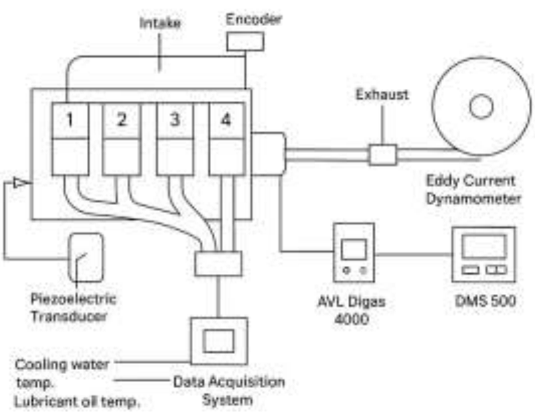

Figure 1: Schematic view of the engine test bed.

Figure 1 presents the schematic experimental setup, which employed a water-cooled, four-cylinder SI port-injection gasoline engine (specifications in Table 1) coupled to an eddy-current dynamometer for torque and speed control. Cylinder pressure was measured using a Kistler 5018 transducer, synchronized with a shaft encoder and charge amplifier, and analyzed via a Combi RT system. Particulate mass, number, and size distribution (5–1000 nm) were obtained using a Cambustion DMS 500 spectrometer, while exhaust emissions (NOx, HC, CO, CO_2) were measured with an AVL Digas 4000 analyzer.

Table 1. Specifications of the test gasoline engine.

Cylinders	Four in a row
Injection type	Aspirate port fuel injection
Bore x stroke / mm	75.0 x 84.8
Connecting road length / mm	143.70
Compression ratio	10.50:1
Work order	1-3-4-2
Rated power /(kw/rpm)	78/6000
Rated torque /(N.m/rpm)	135/4500
The intake valve open /^{o}CA ATDC	353

For this investigation, a commercial gasoline, designated as HE0, served as the base fuel. A test fuel, labeled HE10, was subsequently blended by introducing 10% by volume of hydrous ethanol into the base fuel. The hydrous ethanol was prepared by mixing 5% volumetric water with anhydrous ethanol prior to its addition. The key physical and chemical properties of both the base gasoline and the hydrous ethanol are summarized in Table 2.

Table 2. Properties of gasoline and hydrous ethanol [1]

Property	Unit	Gasoline	Hydrous ethanol
Water content	%vol/vol	0	4.0-5.0
Latent heat of vaporization	kJ/kg	380-500	948
Lower heating value	MJ/kg	43.4	24.76
Stoichiometric air - fuel ratio	w/w	14.7	8.7
Motor octane number	-	80-90	103.3
Carbon	mass%	87.4	50.59
Hydrogen	mass%	12.6	12.89
Oxygen	mass%	0	36.42
Sulphur	ppm	9	0

2.2.2 Operating conditions and procedure

Engine tests were conducted under steady-state conditions at 1800 rpm to assess the effects of hydrous ethanol–gasoline blends on combustion, particulate number, mass, and size distribution as a function of load. Gaseous emissions were measured across 10–50 Nm at 1800 rpm and 40 Nm. For each condition, the engine was warmed to 80 °C with gasoline, residual fuel was purged before switching, and 200 cycles of pressure data were averaged. PM was measured over two minutes, while gaseous emissions were recorded three times and averaged.

3. Results and Discussions:

3.1 Numerical Results

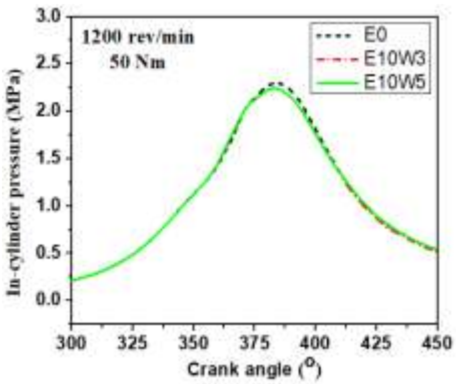

Figure 2: Differences of different water content in ethanol on the in-cylinder pressure.

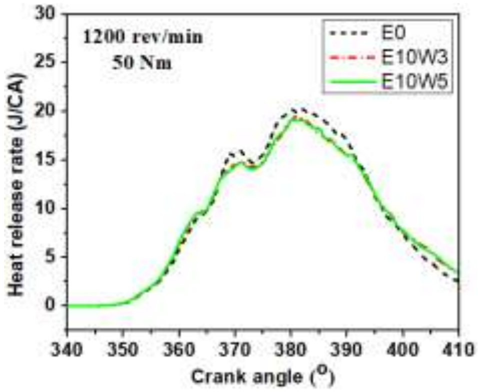

Figure 3: Differences of different water content in ethanol on the heat release rate.

Figures 2 and 3 compare in-cylinder pressure and heat release rate for E0 (100% gasoline), E10W3 (3% water), and E10W5 (5% water) at 1200 rpm and 50 Nm. E0 produced the highest peak pressure and heat release rate, attributed to lower intake manifold pressure and the cooling effect of water in ethanol blends, which reduces in-cylinder temperature. No significant differences were observed between E10W3 and E10W5, likely due to the small water content.

Figure 4 shows that NOx emissions decrease with the addition of water to ethanol blends compared to gasoline, due to lower in-cylinder temperatures that suppress NOx formation. These findings are consistent with previous study [6].

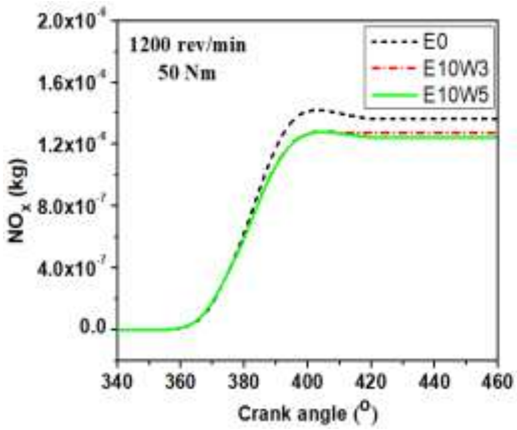

Figure 4: Differences of different water content in ethanol on the NOx emission.

3.2 Experimental Results

Figure 5 compares in-cylinder pressures and heat release rates for HE0 (100% gasoline) and HE10 (10% hydrous ethanol with 5% water) at 1800 rpm under 50 Nm load. HE0 exhibited higher peak pressure and heat release rates than HE10, due to the higher latent heat of vaporization and lower heating value of the hydrous ethanol blend. The increased octane number of HE10 could enhance in-cylinder pressure if compression ratio or ignition timing were adjusted.

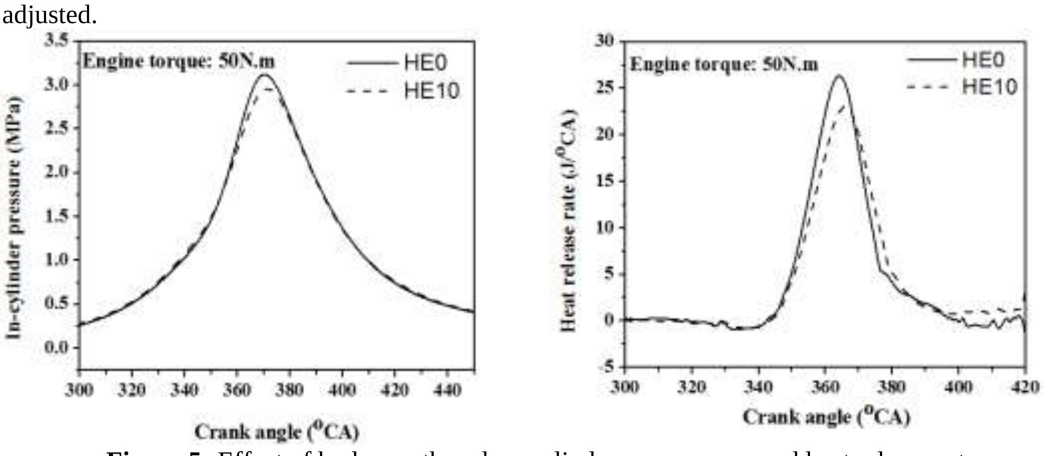

Figure 5: Effect of hydrous ethanol on cylinder gas pressure and heat release rate.

Figure 6 presents the exhaust particulate number (PN) and size distributions for gasoline (HE0) and 10% hydrous ethanol–gasoline (HE10) at 1800 rpm under varying engine loads. PM emissions in the 5–1000 nm range were measured using a DMS 500. Most particles were below 10 nm, with gasoline producing the highest concentrations for particles under 110 nm. Both nucleation and accumulation mode particle concentrations decreased with increasing load for both fuels. HE10 exhibited significantly lower PN than HE0 across 10–50 Nm, attributed to its high oxygen content and absence of aromatics, which reduce particle formation. The addition of ethanol lowers the aromatic content, further decreasing accumulation mode particles. In contrast, HE0 generated a higher number of nucleation mode particles than gasoline, consistent with previous studies [29-31].

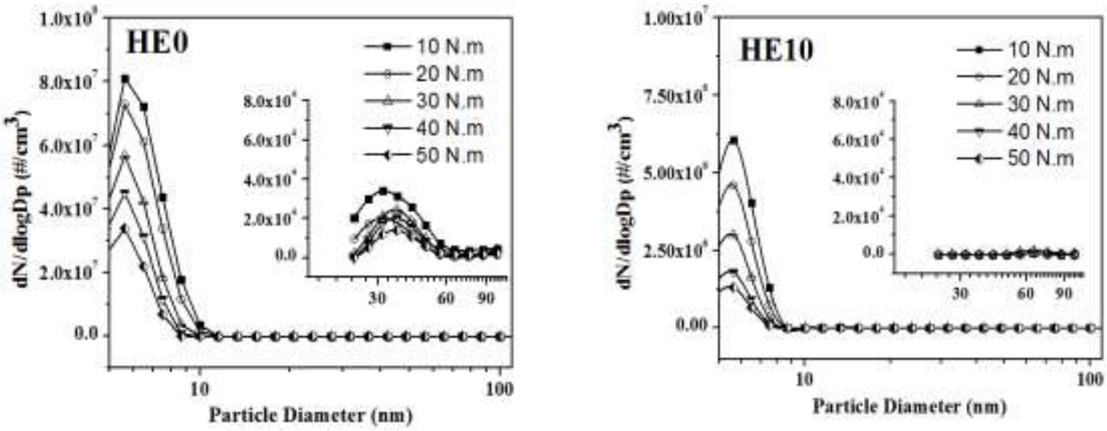

Figure 6: Effects of hydrous ethanol the size distribution under different engine loads.

Figure 7 illustrates the total particle number and mass concentrations at 1800 rpm for engine loads ranging from 10 N·m to 50 N·m. As load increases, total particle number decreases for both fuels due to higher combustion temperatures promoting particle oxidation. HE10 shows lower particle concentrations than HE0. Previous study [32] indicate that particulate emissions in SI engines strongly depend on fuel aromatics and oxygen content. At 30 N·m and 1800 rpm, HE10 reduced particle number by 63.2%.

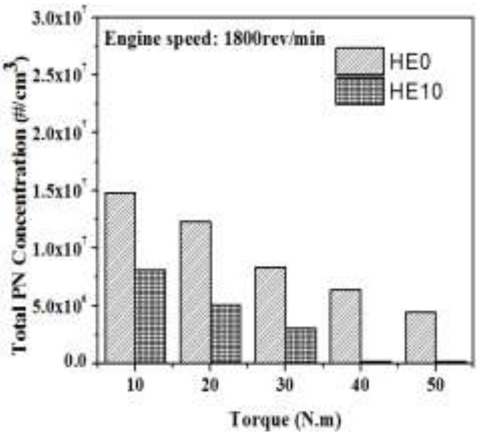

Figure 7: Comparison of particulate number concentrations under different engine loads

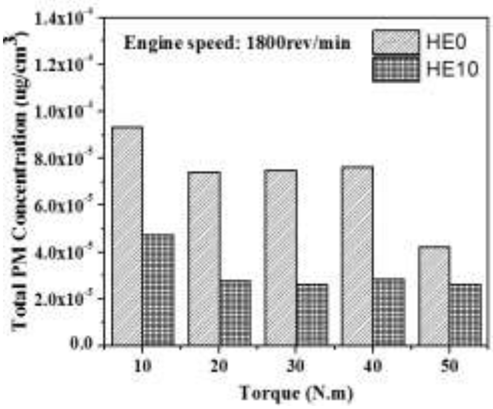

Figure 8: Comparison of total PM concentration under different engine loads.

The results presented in Fig. 8 indicate that particulate mass decreases with increasing engine load for both HE0 and HE10 fuels. This reduction can be attributed to factors similar to those affecting particle number concentration, including reduced aromatic content and the substantially lower carbon fraction of hydrous ethanol 50.59% compared with gasoline 87%, as shown in Table 2. Overall, the HE10 blend achieved a marked improvement, with particulate mass reduced by 64.9% at a load of 30 N•m relative to HE0.

Figure 9 illustrates that HC emissions decline as engine load, primarily due to the rise in in-cylinder temperature. When compared with gasoline, the HE10 blend achieved a 20% reduction in HC emissions at 30 N·m and 1800 rpm. This improvement is attributed to the oxygen content of hydrous ethanol, which enhances combustion efficiency and thereby lowers HC formation.

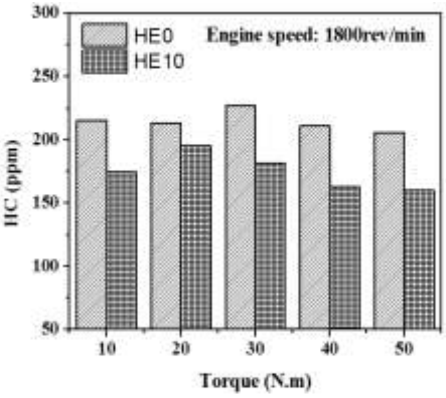

Figure 9: Comparison of HC emission under different engine loads and speeds

Figure 10 illustrates CO and CO_2 emissions at 1800 rpm across loads ranging from 10 to 50 N·m. CO emissions decreased with increasing load, with the HE10 blend showing significant reductions (44.8% at 30 N·m, 1800 rpm). This reduction is primarily attributed to the higher oxygen content of hydrous ethanol, which promotes more complete combustion, and the additional OH radicals generated that enhance CO oxidation. In contrast, CO_2 emissions for HE10 were slightly lower than those for gasoline, reflecting its lower C/H ratio, with a reduction of 4.42% under the same operating condition.

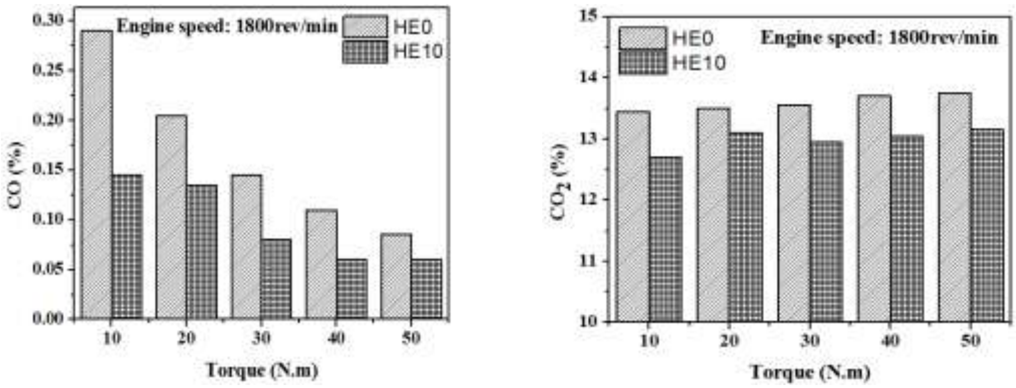

Figure 10: Comparison of (a) CO and (b) CO_2 emissions under different engine loads.

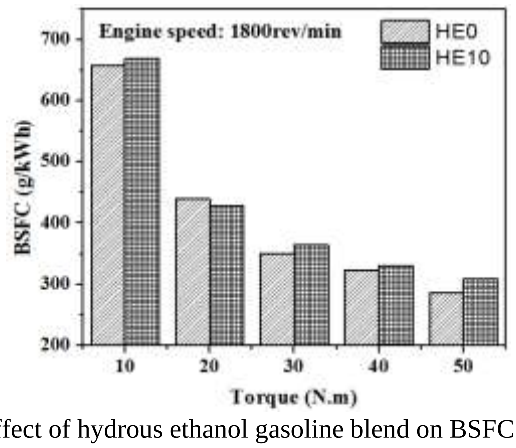

Figure 11: The effect of hydrous ethanol gasoline blend on BSFC at different loads

Figure 11 illustrates the variation of brake specific fuel consumption (BSFC) with engine load. Compared with gasoline, HE10 increased SFC by 4% at 30 N•m and 1800 rpm. This increase is mainly attributed to the lower heating value and higher density of hydrous ethanol blends, requiring greater fuel input to maintain equivalent power.

4. Conclusions

The numerical and experimental investigation of a spark-ignition engine fueled with gasoline and 10% hydrous ethanol–gasoline blend led to the following findings:

- Hydrous ethanol–gasoline blends reduce in-cylinder pressure and heat release compared to gasoline.
- Engine load and fuel type have strong effects on combustion and emissions.
- HE10 demonstrated clear environmental benefits by reducing PM, NOx, HC, CO, and CO_2.
- Particle number and mass concentrations were markedly lower for HE10, improving air quality potential.
- While HE10 does lead to a slight increase in Brake-Specific Fuel Consumption (BSFC), it remains a practical and eco-friendly alternative to conventional gasoline.

Acknowledgement

The authors gratefully acknowledge Professor Maji Luo at the Hubei Key Laboratory of Advanced Technology for Automotive Components and the Hubei Collaborative Innovation Center for Automotive Components Technology, Wuhan University of Technology, for their support during this research.

Compliance with ethical standards

Disclosure of conflict of interest

The authors declare that they have no conflict of interest.

References

[1] M. O. El-Faroug, F. Yan, M. Luo, and R. Fiifi Turkson, “Spark ignition engine combustion, performance and emission products from hydrous ethanol and its blends with gasoline,” *Energies,* vol. 9, no. 12, pp. 984, 2016.

[2] I. Schifter, L. Diaz, J. Gómez, and U. Gonzalez, “Combustion characterization in a single cylinder engine with mid-level hydrated ethanol–gasoline blended fuels,” *Fuel,* vol. 103, pp. 292-298, 2013.

[3] R. Leng, C. Wang, C. Zhang, D. Dai, and G. Pu, “Life cycle inventory and energy analysis of cassava-based fuel ethanol in China,” *Journal of Cleaner Production,* vol. 16, no. 3, pp. 374-384, 2008.

[4] R. C. Clemente, E. Werninghaus, E. P. Coelho, and L. A. S. Ferraz, *Development of an internal combustion alcohol fueled engine,* 0148-7191, SAE Technical Paper, 2001.

[5] K. M. Rahman, N. Kawahara, K. Tsuboi, and E. Tomita, “Combustion characteristics of wet ethanol ignited using a focused Q-switched Nd: YAG nanosecond laser,” *Fuel,* vol. 165, pp. 331-340, 2016.

[6] M. Luo, M. O. El-Faroug, F. Yan, and Y. Wang, “Particulate matter and gaseous emission of hydrous ethanol gasoline blends fuel in a port injection gasoline engine,” *Energies,* vol. 10, no. 9, pp. 1263, 2017.

[7] R. E. Reynolds, “Fuel specifications and fuel property issues and their potential impact on the use of ethanol as a transportation fuel,” *Oak Ridge National Laboratory, Oak Ridge TN USA*, 2002.

[8] S. C. Fang, A. Cassidy, and D. C. Christiani, “A systematic review of occupational exposure to particulate matter and cardiovascular disease,” *International journal of environmental research and public health,* vol. 7, no. 4, pp. 1773-1806, 2010.

[9] C.-L. Myung, A. Ko, Y. Lim, S. Kim, J. Lee, K. Choi, and S. Park, “Mobile source air toxic emissions from direct injection spark ignition gasoline and LPG passenger car under various in-use vehicle driving modes in Korea,” *Fuel processing technology,* vol. 119, pp. 19-31, 2014.

[10] A. Valavanidis, K. Fiotakis, and T. Vlachogianni, “Airborne particulate matter and human health: toxicological assessment and importance of size and composition of particles for oxidative damage and carcinogenic mechanisms,” *Journal of Environmental Science and Health, Part C,* vol. 26, no. 4, pp. 339-362, 2008.

[11] S. Samuel, A. Hassaneen, D. Morrey, and R. Gonzalez-Oropeza, *The Effect of Gasoline Additives on Combustion Generated Nano-scale Particulates,* 0148-7191, SAE Technical Paper, 2009.

[12] J. B. Heywood, “Combustion engine fundamentals,” *1ª Edição. Estados Unidos*, vol. 25, pp. 1117-1128, 1988.

[13] S. No, J. Gu, H. Moon, C. Lee, and Y. Jo, "An introduction to combustion concepts and applications," *McGraw-Hill Korea*, 2011.
[14] W. H. Organization, "World Health Organization Air Quality Guidelines Global Update. 2005," *Geneva, Switzerland: World Health Organization*, 2006.
[15] I. C. Change, "The physical science basis," 2013.
[16] Y. Wang, M. Luo, and M. O. El-Faroug, "The influence of hydrous ethanol gasoline on cycle-to-cycle variation of a spark ignition engine," *Thermal Science,* vol. 22, no. 3, pp. 1373-1384, 2018.
[17] C. H. Rufino, W. L. Gallo, and J. V. Ferreira, "Diagnosis of hydrous ethanol combustion in a spark-ignition engine," *Proceedings of the Institution of Mechanical Engineers, Part D: Journal of Automobile Engineering,* vol. 235, no. 1, pp. 245-259, 2021.
[18] W. Ambrós, T. Lanzanova, J. Fagundez, R. Sari, D. Pinheiro, M. Martins, and N. Salau, "Experimental analysis and modeling of internal combustion engine operating with wet ethanol," *Fuel,* vol. 158, pp. 270-278, 2015.
[19] F. Catapano, S. Di Iorio, P. Sementa, and B. M. Vaglieco, *Characterization of ethanol-gasoline blends combustion processes and particle emissions in a GDI/PFI small engine,* 0148-7191, SAE Technical Paper, 2014.
[20] T. C. C. de Melo, G. B. Machado, C. R. Belchior, M. J. Colaço, J. E. Barros, E. J. de Oliveira, and D. G. de Oliveira, "Hydrous ethanol–gasoline blends–Combustion and emission investigations on a Flex-Fuel engine," *Fuel,* vol. 97, pp. 796-804, 2012.
[21] X. Shi, Y. Jiang, Q. Wang, W. Qian, R. Huang, and J. Ni, "Three-dimensional simulation analysis of the effect of hydrous ethanol and exhaust gas recirculation on gasoline direct injection engine combustion and emissions," *Journal of Energy Resources Technology,* vol. 144, no. 8, pp. 082304, 2022.
[22] F. P. Martins, and P. T. Lacava, "Numerical study of spark plug electrode gap influence of in-cylinder ethanol flame propagation," *Journal of the Brazilian Society of Mechanical Sciences and Engineering,* vol. 46, no. 7, pp. 442, 2024.
[23] A. Willems, P. Rahnama, B. Somers, and R. Novella, "A Numerical Study of Fuel Stratification, Heat Transfer Loss, Combustion, and Emissions Characteristics of a Heavy-Duty RCCI Engine Fueled by E85/Diesel."
[24] J. Gandolfo, B. Lawler, and B. Gainey, "Effect of injection timings and injection pressure on knock mitigation with a compression stroke injection of hydrous ethanol in spark ignition," *International Journal of Engine Research,* vol. 25, no. 11, pp. 1961-1975, 2024.
[25] M. Nazemi, and M. Shahbakhti, "Modeling and analysis of fuel injection parameters for combustion and performance of an RCCI engine," *Applied Energy,* vol. 165, pp. 135-150, 2016.
[26] F. Ibrahim, W. M. F. W. Mahmood, S. Abdullah, and M. R. A. Mansor, *Comparison of simple and detailed soot models in the study of soot formation in a compression ignition diesel engine,* 0148-7191, SAE Technical Paper, 2017.
[27] Y.-D. Liu, M. Jia, M.-Z. Xie, and B. Pang, "Development of a new skeletal chemical kinetic model of toluene reference fuel with application to gasoline surrogate fuels for computational fluid dynamics engine simulation," *Energy & fuels,* vol. 27, no. 8, pp. 4899-4909, 2013.
[28] O. Samimi Abianeh, "Development of a new skeletal chemical kinetic mechanism for ethanol reference fuel," *Journal of Engineering for Gas Turbines and Power,* vol. 137, no. 6, pp. 061501, 2015.
[29] J. M. Storey, T. Barone, K. Norman, and S. Lewis, "Ethanol blend effects on direct injection spark-ignition gasoline vehicle particulate matter emissions," *SAE International Journal of Fuels and Lubricants,* vol. 3, no. 2010-01-2129, pp. 650-659, 2010.
[30] J. M. Storey, T. L. Barone, J. F. Thomas, and S. P. Huff, *Exhaust particle characterization for lean and stoichiometric DI vehicles operating on ethanol-gasoline blends,* 0148-7191, SAE Technical Paper, 2012.
[31] J. Cho, W. Si, W. Jang, D. Jin, C.-L. Myung, and S. Park, "Impact of intermediate ethanol blends on particulate matter emission from a spark ignition direct injection (SIDI) engine," *Applied Energy,* vol. 160, pp. 592-602, 2015.
[32] G. Karavalakis, D. Short, V. Chen, C. Espinoza, T. Berte, T. Durbin, A. Asa-Awuku, H. Jung, L. Ntziachristos, and S. Amanatidis, *Evaluating Particulate Emissions from a Flexible Fuel Vehicle with Direct Injection when Operated on Ethanol and Iso-butanol Blends,* 0148-7191, SAE Technical Paper, 2014.

